SEDIMENTATION OF DREDGED CHANNELS BY CURRENTS AND WAVES

By Leo C. van Rijn[1]

ABSTRACT: A detailed mathematical model for sedimentation of dredged channels, based on a detailed representation of all relevant transport processes such as convection, mixing and settling, is presented. This is an important advantage compared with the traditional prediction formulas, which are based on a rather strong schematization of the transport processes. A sensitivity analysis is presented showing the influence of the streamline refraction effect and the wave shoaling effect in the channel on the sedimentation process. Two applications of the proposed mathematical model are given and show reasonable agreement between measured and computed concentrations and sedimentation rates. Finally, a set of graphs is presented which can be used to get a rough estimate of the trapping efficiency of dredged channels.

INTRODUCTION

Usually, the design of a planned navigation channel requires the determination of: (1) The tracé and alternatives; (2) the channel dimensions depending on vessel sizes, movements, keel clearances, local regulations, sedimentological conditions (stable slopes); and (3) capital and maintenance dredging volumes. A good overview of all relevant aspects and available design methods is given by Van der Weide et al. (22).

This paper focuses on predicting the maintenance dredging volume of various types of channels (e.g., navigation, pipelines, tunnels). Since dredging costs are usually critical to the economic feasibility of the entire project, an important objective of a sedimentation study is to minimize the capital and maintenance dredging costs by studying various design alternatives. This implies a high accuracy of the predicted sedimentation rates.

Basically, an accurate sedimentation prediction requires a detailed field survey to determine the boundary conditions such as: current velocities; streamline patterns; wave characteristics; salinities; size, composition and porosity of bed material; sediment concentrations; particle fall velocities of suspended sediments and effective bed roughness. Further improvement of the accuracy can be obtained by carrying out a trial dredge investigation. Such an investigation can be considered necessary when the costs of the capital and maintenance dredging values of the planned channel are relatively large compared with those of the trial dredge channel. The sedimentation rates observed in the trial dredge channel can be used to check or calibrate the available prediction methods resulting in a more accurate sedimentation prediction.

In preceding years, a large number of simple prediction methods have been proposed to compute the sedimentation rate of a channel (3,4,11,12).

[1]Sr. Research Engr., Delft Hydraulics Lab., P.O. Box 152, Emmeloord, The Netherlands.

Note.—Discussion open until February 1, 1987. To extend the closing date one month, a written request must be filed with the ASCE Manager of Journals. The manuscript for this paper was submitted for review and possible publication on September 10, 1985. This paper is part of the *Journal of Waterway, Port, Coastal and Ocean Engineering*, Vol. 112, No. 5, September, 1986. ©ASCE, ISSN 0733-950X/86/0005-0541/$01.00. Paper No. 20883.

A disadvantage of these simple methods is the rather strong schematization of the relevant transport processes. Preferably, the simple methods should be used only when trial dredge results are available to calibrate the empirical coefficients or when a rough estimate of the sedimentation rate is considered adequate. A more reliable prediction can be expected when a detailed mathematical model representing the relevant transport processes, is applied. A mathematical model can also be used with greater confidence outside its verification range. In this paper, a two-dimensional vertical mathematical model for suspended sediment transport by current and waves is proposed. A similar model for currents alone has already been presented (9,10,14). A brief description of the model (SURTRENCH) is presented. After that, a sensitivity analysis is presented showing the influence of the current refraction effect and the wave shoaling effect in the channel on the sedimentation process. Two applications are given: a flume experiment, and a field investigation. Finally, a set of graphs is presented, which can be applied to get a rough estimate of the trapping efficiency of a dredged channel.

Mathematical Model

Sediment Transport Processes.—When a current passes over a dredged channel, the sediment transport capacity decreases and some of the suspended sediment particles is deposited in the channel. The most relevant processes which should be represented are: the convection of the particles by the horizontal and vertical fluid velocities; the diffusion or mixing of the particles due to the current-related and wave-related mixing processes; the settling of the particles due to gravity; and the pick-up of the particles from the bed by the flow as shown schematically in Fig. 1.

Basic Equations for Sediment Concentrations.—The computation of the concentrations is based on a numerical solution of the convection-diffusion equation. Assuming steady state conditions and neglecting the transport by longitudinal mixing, which is relatively small (10), the convection-diffusion equation for the wave period-averaged variables can be expressed as:

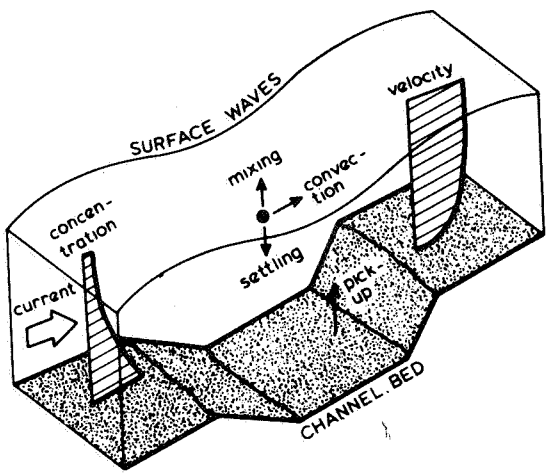

FIG. 1.—Sedimentation in Dredged Channel

$$\frac{\partial}{\partial x}(buc) + \frac{\partial}{\partial z}[b(w - w_s)\,c] - \frac{\partial}{\partial z}\left(b\epsilon_{s,cw}\frac{\partial c}{\partial z}\right) = 0 \quad \ldots\ldots (1)$$

in which u = longitudinal velocity at height z above the bed; c = sediment concentration; w = vertical flow velocity; w_s = particle fall velocity of suspended sediment; $\epsilon_{s,cw}$ = sediment mixing coefficient by current and waves; b = flow width; x = longitudinal coordinate; and z = vertical coordinate. By varying the flow width (b), a gradually diverging or converging flow can be represented. The flow velocities and sediment concentrations are assumed to be constant in lateral direction. The flow width as a function of distance must be known a priori (field survey, physical scale model or mathematical model) and specified to the SURTRENCH-model. Eq. 1 can be solved numerically when the flow velocities, the sediment mixing coefficients and the particle fall velocity are known.

Velocity Profiles.—Since at this stage of research only gradually varying currents in combination with relatively small waves (ratio of wave height and water depth < 0.3) are considered; it seems reasonable to represent the velocity profiles by a simple logarithmic distribution, as follows:

$$u = \frac{u_h}{\ln\left(\frac{h}{z_o}\right)} \ln\left(\frac{z}{z_o}\right) \quad \ldots\ldots (2)$$

$$u_h = \frac{\ln\left(\frac{h}{z_o}\right)}{-1 + \ln\left(\frac{h}{z_o}\right)}\left[\frac{Q}{bh}\right] \quad \ldots\ldots (3)$$

in which u = longitudinal flow velocity; u_h = water surface velocity; h = water depth; Q = discharge; z = height above bed; $z_o = 0.33k_s$ = zero-velocity level; and k_s = effective roughness height. The vertical velocity (w) can be computed from the fluid continuity equation, as follows:

$$w = -\int_{z_o}^{z} \frac{\partial u}{\partial x}\,dz - \frac{1}{b}\frac{db}{dx}\int_{z_o}^{z} u\,dz \quad \ldots\ldots (4)$$

yielding a rather simple analytic expression. The bed-shear velocity (u_*) follows from (see Eq. 2):

$$\frac{u_h}{\ln\left(\frac{h}{z_o}\right)} = \frac{u_*}{\kappa} \quad \ldots\ldots (5)$$

Substitution of Eq. 3 in Eq. 5 results in:

$$u_* = \frac{\kappa}{-1 + \ln\left(\frac{h}{z_o}\right)}\frac{Q}{bh} \quad \ldots\ldots (6)$$

in which κ = constant of Von Karman.

Mixing Coefficients.—The mixing coefficient for current and waves is represented by a linear combination of the current-related and the wave-related mixing coefficient, as follows:

$$\epsilon_{s,cw} = \epsilon_{s,c} + \epsilon_{s,w} \quad \ldots\ldots (7)$$

in which $\epsilon_{s,c}$ = current-related sediment mixing coefficient and; $\epsilon_{s,w}$ = wave-related mixing coefficient.

The current-related mixing coefficient is described by (see also Fig. 2):

$$\epsilon_{s,c} = \epsilon_{s,c,\max} - \epsilon_{s,c,\max}\left(1 - \frac{2z}{h}\right)^{\eta} \quad \text{for} \quad \frac{z}{h} < 0.5 \quad \ldots\ldots (8a)$$

$$\epsilon_{s,c} = \epsilon_{s,c,\max} = 0.25\,\beta\kappa u_{*,c} h \quad \text{for} \quad \frac{z}{h} \geq 0.5 \quad \ldots\ldots (8b)$$

in which $u_{*,c}$ = current-related bed-shear velocity according to Eq. 6; β = ratio of sediment and fluid mixing coefficient; and η = coefficient. The η-coefficient was determined by calibration using measured concentration profiles for flow superimposed by waves (19), yielding:

$$\eta = -0.25\frac{\hat{u}_{b,w}}{|\bar{u}|} + 2 \quad \text{for} \quad 0 \leq \frac{\hat{u}_{b,w}}{|\bar{u}|} \leq 4 \quad \ldots\ldots (9a)$$

$$\eta = 1 \quad \text{for} \quad \frac{\hat{u}_{b,w}}{|\bar{u}|} > 4 \quad \ldots\ldots (9b)$$

in which $\hat{u}_{b,w}$ = peak value of orbital velocity at bed according to linear wave theory, $\bar{u}$ = cross-section averaged velocity.

Eq. 9 yields η-values in the range from 1–2. For conditions without waves ($\hat{u}_{b,w} = 0$) it follows that $\eta = 2$, which means a parabolic distribution of the mixing coefficient in the lower half of the water depth. The wave-related mixing coefficient is described by (see also Fig. 2):

$$\epsilon_{s,w} = \epsilon_{s,w,\text{bed}}, \quad \text{for} \quad z \leq \delta \quad \ldots\ldots (10a)$$

$$\epsilon_{s,w} = \epsilon_{s,w,\max}, \quad \text{for} \quad z \geq 0.5\,h \quad \ldots\ldots (10b)$$

$$\epsilon_{s,w} = \epsilon_{s,w,\text{bed}} + (\epsilon_{s,w,\max} - \epsilon_{s,w,\text{bed}})\left(\frac{z-\delta}{0.5\,h - \delta}\right), \quad \text{for} \quad \delta < z < 0.5\,h \quad \ldots\ldots (10c)$$

in which $\epsilon_{s,w,\text{bed}}$ = wave-related mixing coefficient close to the bed; $\epsilon_{s,w,\max}$ = wave-related mixing coefficient in the upper half of the water depth;

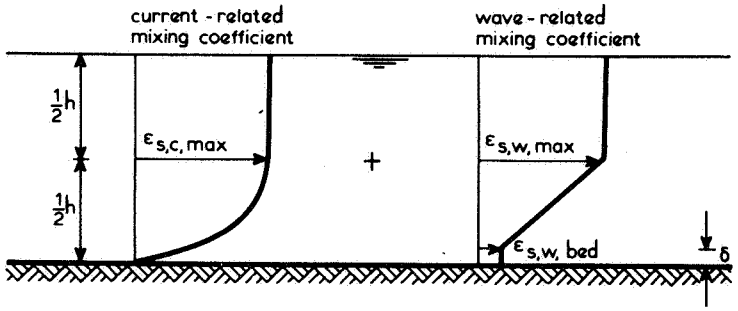

FIG. 2.—Vertical Distribution of Sediment Mixing Coefficient

and δ = thickness of near-bed mixing layer ($\simeq$ three times the ripple height, 19).

Eq. 10 is based on the analysis of measured concentration profiles for waves alone. The characteristic parameters of the mixing coefficient distribution were related to general wave parameters (19), yielding:

$$\epsilon_{s,w,\text{bed}} = \alpha_1 \delta \hat{u}_{b,w} \quad \ldots\ldots (11)$$

$$\epsilon_{s,w,\max} = \alpha_2 \frac{hH_s}{T_s} \quad \ldots\ldots (12)$$

in which H_s = significant wave height; T_s = significant wave period (relative to coordinate system moving with the current); $\alpha_1 = 0.00065\ D_*^2$ = coefficient; $\alpha_2 = 0.035$ = coefficient, $D_* = D_{50}\ (\Delta g/\nu^2)^{1/3}$ = particle parameter, $\Delta = (\rho_s - \rho)/\rho$ = relative density; ρ_s = sediment density; ρ = fluid density; g = acceleration of gravity; ν = kinematic viscosity coefficient; and D_{50} = median particle size of bed material.

Boundary Conditions.—The following specifications are required:

Flow Domain.—Initial bed levels, water depth, flow widths, wave characteristics, particle fall velocity, effective bed roughness, size, composition and porosity of bed material.

Inlet Boundary.—Discharge, flow velocities, mixing coefficients, concentrations.

Water Surface.—Net vertical transport is assumed to be zero.

Bed Surface.—Bed concentration or upward sediment flux at bed as a function of local hydraulic and sediment parameters.

The bed-boundary condition is specified at a small height ($z = a$) above the mean bed. Using this approach, the bed concentration or the sediment flux can be represented by its equilibrium value assuming that there is an almost instantaneous adjustment to equilibrium conditions close to the bed.

For equilibrium conditions the author has proposed the following bed-concentration function (15,16,17,19):

$$c_a = \alpha \frac{D_{50}}{a} \frac{T^{1.5}}{D_*^{0.3}} \quad \ldots\ldots (13)$$

in which c_a = bed-boundary concentration; a = reference level above bed; $T = (\bar{\tau}'_{b,cw} - \bar{\tau}_{b,\text{cr}})/\bar{\tau}_{b,cr}$ = bed-shear stress parameter; $\bar{\tau}'_{b,cw} = \mu_c \bar{\tau}_{b,c} + \mu_w \bar{\tau}_{b,w}$ = effective bed-shear stress; $\bar{\tau}_{b,c}$ = current-related bed-shear stress; $\bar{\tau}_{b,w}$ = wave-related bed-shear stress according to linear wave theory (based on significant wave height, length and period); μ_c = current-related efficiency factor; $\mu_w = 0.8/D_*$ = wave-related efficiency factor; $\bar{\tau}_{b,\text{cr}}$ = critical bed-shear stress according to Shields; and $\alpha = 0.015$ = coefficient. Eq. 13, originally proposed for currents alone, was recalibrated for currents superimposed by waves using additional flume and field data (19). The upward sediment flux at the bed is defined as:

$$E_a = -\left(\epsilon_s \frac{\partial c}{\partial z}\right)_{z=a} = w_s c_a = \alpha\, w_s \frac{D_{50}}{a} \frac{T^{1.5}}{D_*^{0.3}} \quad \ldots\ldots (14)$$

Eqs. 13 and 14 are both implemented in the SURTRENCH-model. Either

Eq. 13 or Eq. 14 can be selected (input parameter). A sensitivity analysis has shown that both functions yield approximately the same sedimentation rates (18).

Bed Level Computation.—Bed level changes are computed from the cross-section integrated sediment continuity equation, which reads:

$$\frac{\partial}{\partial t}(bz_b) + \frac{1}{\rho_s(1-p)}\frac{\partial}{\partial x}(S_s + S_b) = 0 \quad \ldots\ldots (15)$$

in which t = time; b = flow width; z_b = bed level above a horizontal datum; p = porosity factor; S_s = suspended load transport; and S_b = bed load transport. The suspended load transport is computed as:

$$S_s = b\int_a^h ucdz \quad \ldots\ldots (16)$$

The bed-load transport is described by a simple formula (19):

$$S_b = 0.1\, bD_{50}\, u'_{*,c}\frac{T^{1.5}}{D_*^{0.3}} \quad \ldots\ldots (17)$$

Numerical Solution Methods.—To solve Eq. 1, a finite-element method based on weighted residuals according to the (modified) Galerkin-method is used (21). The continuous two-dimensional solution domain is divided into a system of quadrangular elements. The vertical dimension of the elements decreases toward the bed to provide a greater resolution in the near-bed region where large velocity and concentration gradients exist. Between the nodes of the elements the unknown variable is represented by a linear function. Then, for each element, the coefficients corresponding to the unknown variable at each node are determined. Finally, the tri-diagonal coefficients matrix for the complete domain is determined, from which the coefficients can be solved. In the vertical direction, at least 10 nodal points are necessary for an accurate representation of the concentration profiles.

The computations are carried out on a CDC Cyber 855 computer with a maximum memory of 400 K words. One time step for a grid of 50 × 10 points takes about 1.5 sec CPU time.

Channels Oblique to Approaching Current

Generally, sedimentation predictions have to be made for channels which are oblique to the approaching current. When a steady current approaches an oblique channel, the streamlines of the current are refracted at the upstream and downstream side slopes of the channel. The refraction effect is largest near the bed and smallest near the water surface. Because of the refraction effect, the streamlines are contracted within the channel resulting in an increase of the velocities. For reasons of continuity, however, the velocities in the channel decrease due to the increase of the water depth. Depending on which of these effects is stronger, the current velocities in the channel can be smaller or larger than the velocities of the approaching current. Usually, there is an overall increase of the velocities in the channel when the angle between the ap-

proaching current and the channel axis is smaller than about 20°. For an oblique channel of infinite length the depth-averaged current velocity can be described by the following equations:

$$\textit{continuity:}\quad \frac{\partial}{\partial x}(h\bar{u}) = 0 \qquad (18)$$

$$\textit{motion:}\quad \bar{u}\frac{\partial \bar{u}}{\partial x} + \frac{1}{\rho}\frac{\partial \bar{p}}{\partial x} + \frac{\bar{\tau}_{b,x}}{\rho h} - g s_x = 0 \qquad (19a)$$

$$\bar{u}\frac{\partial \bar{v}}{\partial x} + \frac{\bar{\tau}_{b,y}}{\rho h} - g s_y = 0 \qquad (19b)$$

in which: $\bar{u}$, $\bar{v}$ = depth-averaged velocities in x- and y-directions; $\bar{p}$ = depth-averaged fluid pressure; $\bar{\tau}_b$ = mean bed-shear stress; s_x, s_y = bottom gradients in x- and y-directions; h = water depth; ρ = fluid density; and g = acceleration of gravity.

Boer (2) has shown that the convection terms as well as the friction terms are of essential importance for a good representation of the flow field. Boer has also given a simple numerical solution of Eqs. 18 and 19 which allows the depth-averaged velocities and the local current direction to be computed. Knowing the current velocities along the refracted streamlines, these values can be specified to the SURTRENCH-model by varying the width (stream tube approach), and the concentration profiles can then be computed.

Sensitivity Analysis

A detailed sensitivity analysis has been carried out to identify the influence of the controlling parameters on the computed sedimentation rates (18). Based on this investigation, the main controlling parameters were found to be: the current; wave and sediment transport conditions at the inlet ($x = 0$); the particle fall velocity of the suspended sediments; the direction of the approaching current in relation to the streamline refraction effect; and the wave height variations across the channel (shoaling effect). This paper focuses on the influence of the streamline refraction effect and the influence of wave height variations across the channel. Information of the influence about the boundary conditions at the inlet ($x = 0$) and the influence of the particle fall velocity has been given by Kerssens et al. (10) and Van Rijn (14). The main conclusion is that the application of a mathematical model is only meaningful when detailed and accurate information of the boundary conditions (field measurements in combination with mathematical forecasts) is available. In the absence of such data, simple sedimentation formulas or graphs should be used to get a rough estimate of the sedimentation rate.

Influence of Streamline Refraction.—To investigate the influence of the refraction effect, computations were carried out for refracted and unrefracted streamlines, as shown schematically in Fig. 3.

Various approach angles were considered. The other boundary conditions were the same for all computations. The wave height was assumed to be constant in the computation domain. The current velocities

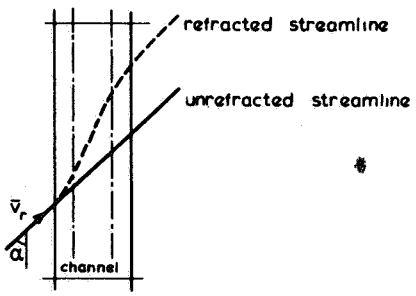

FIG. 3.—Refracted and Unrefracted Streamlines

along the refracted streamlines were computed numerically applying Eqs. 18 and 19, which are valid for a channel of infinite length. The influence of the waves on the streamline refraction has been neglected. The computed current velocities were specified to the SURTRENCH model by varying the width along the streamlines (stream tube approach). Similar SURTRENCH computations were carried out for the unrefracted streamlines. In the latter case the mean current velocity at each location is inversely proportional to the local water depth. Fig. 4 shows the current direction (α), the current velocity vector ($\bar{v}_r$), the suspended load transport (S_s) integrated over the cross-section of the streamtube and the bed levels for an approach angle of $\alpha_o = 10°$. The bed levels have been computed over a period of 10 days for a symmetrical tidal flow which is represented as two quasi-steady periods of 4 hours each.

Firstly, the computation for the refracted streamlines is described. The mean current velocity along the refracted steamlines shows an increase from 1 m/s to 1.35 m/s at the downstream side slope. Because of the increasing velocities, the reduction of the suspended load transport in the channel (resulting in sedimentation) is relatively small and is mainly caused by the lateral contraction of the streamlines. Downstream of the channel axis the suspended load transport increases resulting in erosion. The computed bed level profile shows no sedimentation in the middle of the channel because the sedimentation during the ebb (or flood) period is removed during the flood (or ebb) period. Based on this result, it seems that a channel oblique to the current at a small angle of 10° would be self-cleansing. The self-cleansing effect has also been found in laboratory experiments for small approach angles (5). In natural conditions, however, the self-cleansing effect has not been observed because of the presence of additional effects such as the infill of bed-load particles due to the gravity component, lateral diffusion, and asymmetrical tidal flow. The computation for the unrefracted streamlines shows a decrease of the current velocity in the channel and, hence, a considerable sedimentation. Fig. 5 shows the results for an approach angle of 60°. As can be observed, the influence of the refraction effect is relatively small for $\alpha_o = 60°$. Consequently, for approach angles larger than 60° it seems quite acceptable to neglect the refraction effect. Finally, note that the sedimentation rate increases for an increasing approach angle (compare Figs. 4 and 5). To reduce the sedimentation rate, the channel axis should be as much as possible parallel to the local current direction.

Influence of Wave Height Variations across Channel.—When waves propagate in a region with a varying water depth, the wave height and

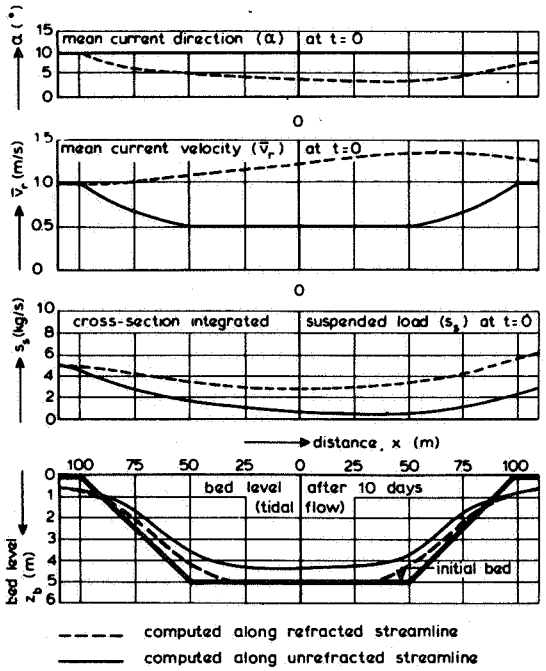

FIG. 4.—Influence of Refraction Effect on Sedimentation in Oblique Channel, α_o = 10° (Tidal Flow); h_o = 5 m; $\bar{v}_{r,o}$ = 1 m/s; H = 2 m; T = 7 s; w_s = 0.015 m/s; $k_{s,w}$ = 0.05 m; and $k_{s,c}$ = 0.05 m

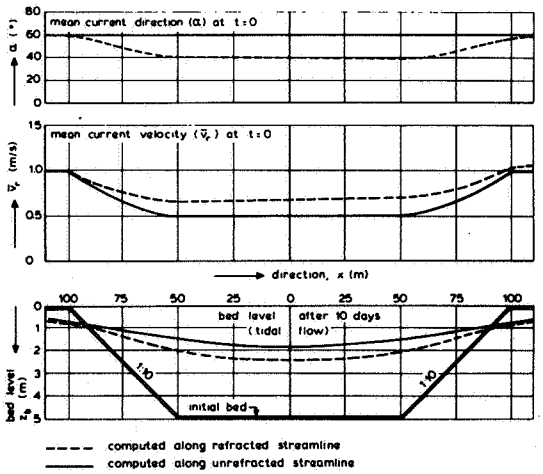

FIG. 5.—Influence of Refraction Effect on Sedimentation in Oblique Channel, α_o = 60° (Tidal Flow)

length are changed. Assuming the wave direction to be parallel to the current direction and neglecting bottom friction and wind input, the wave height variation over a gradually varying bottom can be computed from the conservation law for the energy flux, which reads (6):

$$\frac{d}{dx}\left[\frac{E(\bar{u}+c_{gr})}{\omega_r}\right]=0 \quad \ldots\ldots\ldots\

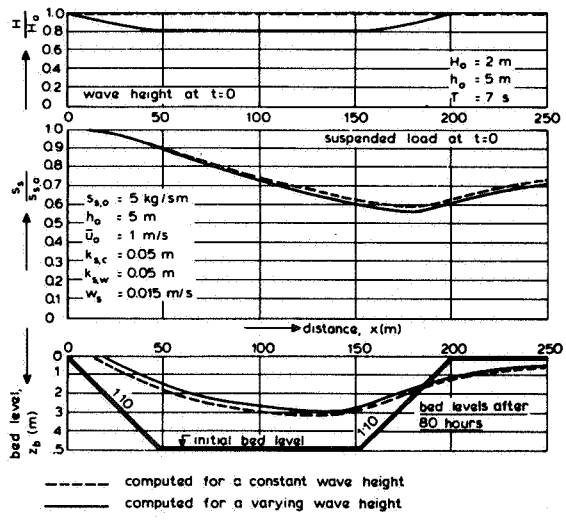

FIG. 6.—Influence of Wave Height on Sedimentation in a Channel Perpendicular to Waves and Current (Unidirectional Flow)

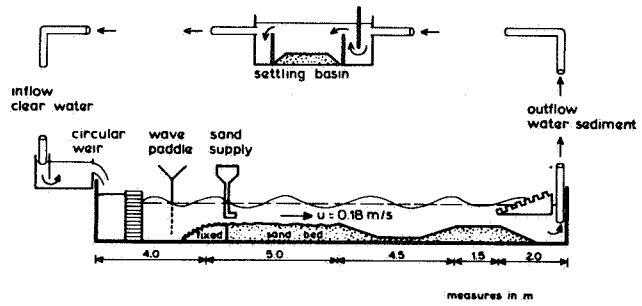

FIG. 7.—Experiment Set-Up

Assuming the absolute wave period and the current velocity to be known, the wave height and length can be computed iteratively. Fig. 6 shows computed wave heights for a channel perpendicular to the wave and current direction. The wave direction was taken opposite to the current direction because this situation yields the largest wave height reduction in the channel (18). The computed suspended load transport at initial time and the bed level changes after 80 hours for a reduced wave height are shown in Fig. 6. Similar computation results for a constant wave height across the channel are also shown in Fig. 6.

As can be observed, the influence of a reduced wave height on the suspended load transport and the bed level changes is rather small. A reduced wave height yields a somewhat larger sedimentation because this condition leads to the reduction of the wave-related mixing and re-entrainment of bed particles in the channel. When the waves and the current are in the same direction, the differences are even smaller than those presented in Fig. 6. Based on these results, it seems acceptable to assume the wave height to be constant inside and outside the channel for most engineering purposes.

VERIFICATION OF SURTRENCH-MODEL

Two verification examples are given: a flume experiment and a field experiment. These verifications are comparisons of predicted and mea-

sured sediment concentrations and bed level changes in the channel assuming all hydraulic conditions (including the sediment transport rate) to be known at the inlet ($x = 0$) of the channel. Thus, the sediment transport rate at $x = 0$ is not predicted by the model but specified to the model as an input parameter. Based on a known sediment transport rate at $x = 0$, the α-coefficient of the bed-boundary condition (Eq. 13 or 14) is determined assuming an equilibrium concentration profile and a logarithmic velocity profile at the inlet. This α-coefficient, which is based on the input values at $x = 0$, is then used to compute the bed concentration or flux at all other locations ($x > 0$).

Flume Experiments.—To evaluate the results of the SURTRENCH-model, a flume (length = 17 m, width = 0.3 m, depth = 0.5 m) experiment was carried out concerning the migration and sedimentation of a channel perpendicular to the current direction. The current and the waves were in the same direction. The experimental set-up is shown in Fig. 7.

Sand was used as bed material (D_{50} = 100 μm, D_{90} = 130 μm). The sand bed had a thickness of about 0.2 m. A channel with side slopes of 1:10 and a depth of 0.125 m was excavated in the measuring section of the flume. A pumping system was used to generate a steady current. The water depth and current velocity upstream of the channel were h_0 = 0.255 m and $\bar{u}_0$ = 0.18 m/s. Regular waves with a period of 1.5 s were generated by a simple wave paddle, which was perforated to allow the passage of the current. The wave height upstream of the channel was 0.08 m. Wave height measurements in the channel showed an irregular pattern with (small) local wave height increases and decreases, probably as a result of secondary waves generated by the wave paddle and the bottom variations in the channel. To maintain equilibrium conditions (no scour or deposition) upstream of the channel, sand of the same size and composition as the bed material was supplied at a constant rate of 0.0167 kg/sm. Ripples with a height in the range of 0.01 to 0.02 m and a length in the range of 0.05 to 0.08 m were generated in the movable bed section. Current velocities were measured by using an acoustical-doppler method. Sand concentrations were determined from water samples collected by use of a siphon system at various locations in the center line of the flume. Analysis of the suspended sand samples showed a variation of the particle size in the range of 110 μm (near the bed) to 80 μm (near the water surface). The corresponding particle fall velocities are in the range of 0.01 m/s to 0.005 m/s (water temperature of 17° C). Detailed information is given by Van Rijn (20).

The SURTRENCH-model was operated with an equilibrium concentration profile at the inlet boundary ($x = 0$) and an upward sediment flux at the bed-boundary ($z = a$) according to Eq. 14. The coefficient of Eq. 14 was adjusted to give the correct suspended load transport rate at the inlet, which means a value equal to the supply rate. The bed-load transport rate could not be measured and was therefore not represented. The current-related bed roughness was found to be about 0.02 m, based on the analysis of velocity profiles measured in the absence of waves (separate tests). To compute the wave-related friction factor, the wave-related bed roughness was assumed to be equal to three times the maximum ripple height (19). This latter value was also used to represent the thickness of the wave-related mixing layer near the bed (δ = 0.06

m). The representative particle fall velocity of the suspended sediment was assumed to be 0.007 m/s. The wave height in the channel was taken equal to that upstream of the channel (H = 0.08 m). The other hydraulic parameters are: ρ_s = 2,650 kg/m^3; ρ = 1,000 kg/m^3; β = 1; κ = 0.4; and p = porosity factor = 0.4. The numerical parameters are: Δx = longitudinal grid size = 0.25 m; Δt = time step = 900 s; and a = reference level = 0.01 m; 10 grid points were used in the vertical direction.

Fig. 8 shows measured and computed velocity and concentration profiles at initial time (t = 0). Comparison of the measured and computed velocity profiles upstream of the channel (profile 1) shows that a loga-

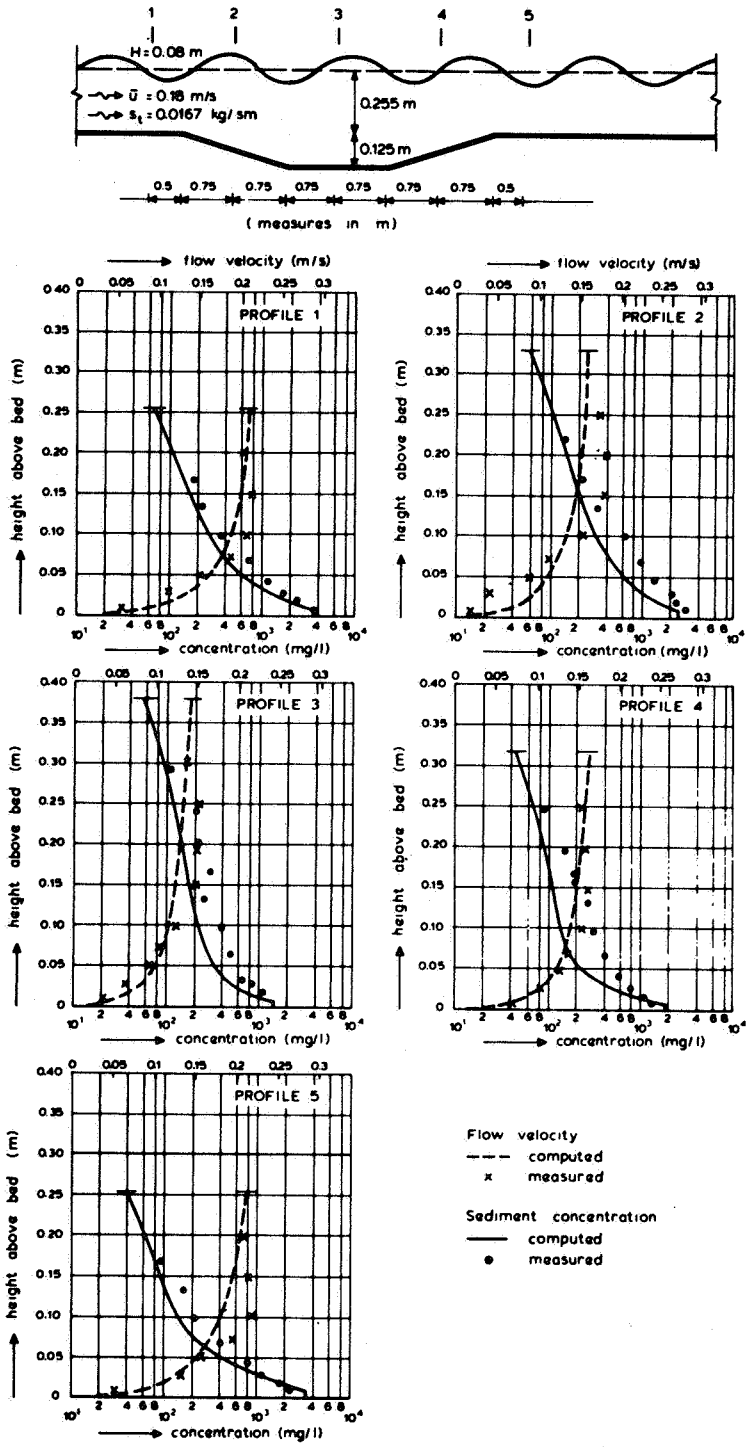

FIG. 8.—Measured and Computed Velocity and Concentration Profiles

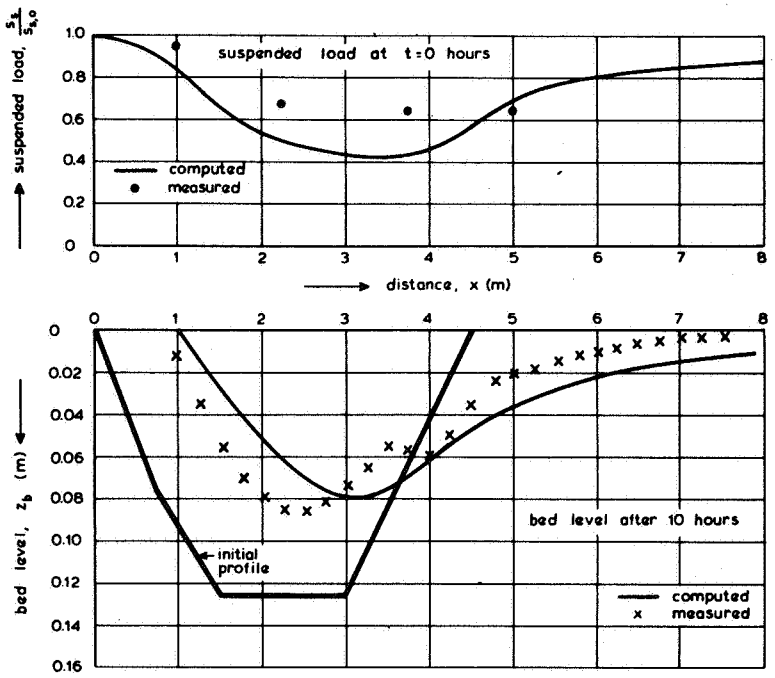

FIG. 9.—Variation of Suspended Load Transport and Bed Levels along Channel

rithmic velocity distribution is not fully satisfactory. It has been shown (1,7,8) that the velocity profile is modified by the waves yielding reduced near-bed and near-surface velocities in the case of a current in the same direction as the waves. This effect has not been represented in the present computations.

Comparison of measured and computed velocity profiles in the deceleration zone of the channel (profile 2) shows relatively large deviations. Evidently, the deceleration effect cannot be represented by a logarithmic velocity distribution. Further research is necessary to improve this. Comparison of measured and computed concentration profiles shows that the computed values are systematically too small. The smallest deviations can be observed in the near-bed region which is an indication of the applicability of Eq. 14 as bed-boundary condition. An acceptable explanation for the underestimation of the measured sand concentrations is the additional turbulence (increased mixing) generated in the deceleration zone of the channel which is not represented in the mathematical model. Because of that, the computed mixing coefficients and, hence, the computed concentrations are too small. Fig. 9 shows the variation of the depth-integrated suspended load transport at initial time ($t = 0$) along the channel and the bed-level changes after 10 hours.

The reduction of the computed suspended load transport is too large compared with "measured" values, the latter being computed from the measured velocity and concentration profiles ($s_s = \int ucdz$). The computed sedimentation and erosion rates are also too large compared with measured values. The measured sedimentation volume in the channel is about 20% smaller than the computed value. Finally, note that a small bar is generated at the downstream side slope as a result of a small local wave height decrease.

In summary, the present results are encouraging, and further research is necessary and should be aimed at improving the current velocities and

the sediment mixing coefficients in the deceleration zone. It is realized that the scale of the present test is rather small. Further tests will be carried out on a larger scale to reduce the generation of secondary waves as much as possible.

Field Experiment.—A trial dredge investigation was carried out in the coastal waters near Bahia Blanca, Argentina (13). The dimensions of the trial dredge channel are shown in Fig. 10. Based on detailed field measurements, the approach angles of the dominant flood and ebb currents were found to be about 5°. Analysis of tidal data showed a mean range of about 2 m. The maximum current velocities were about 0.45 m/s. Analysis of wave data showed a significant wave height of about 0.5 m with a period in the range of 4 to 12 s during 95% of the time. During storm periods the significant wave heights were as large as 2 m with a period of 10 s. Analysis of various bed material samples showed the presence of silty and sandy materials. The sand material had a D_{50} of about 110 μm.

Based on concentration measurements, the depth-averaged concentration was found to be about 85 mg/L consisting of silty (80%) and sandy (20%) materials. In-situ fall velocity measurements showed a characteristic value of about 1 mm/s. The bed profiles inside and outside the channel were almost flat (echo-soundings). Analysis of bed material samples collected inside the channel showed a porosity factor of about 75%!

To operate the SURTRENCH-model, the mean tidal cycle was schematized to 2 quasi-steady flow periods of 6 hours each with characteristic current velocities of 0.3 m/s. A two-dimensional horizontal flow model was operated to compute the depth-averaged current velocities along the refracted streamlines (2). These data were specified to the SURTRENCH-model by varying the flow width (stream tube approach). At the inlet boundary of the SURTRENCH-model equilibrium concentration profiles were assumed to be present with a depth-averaged value

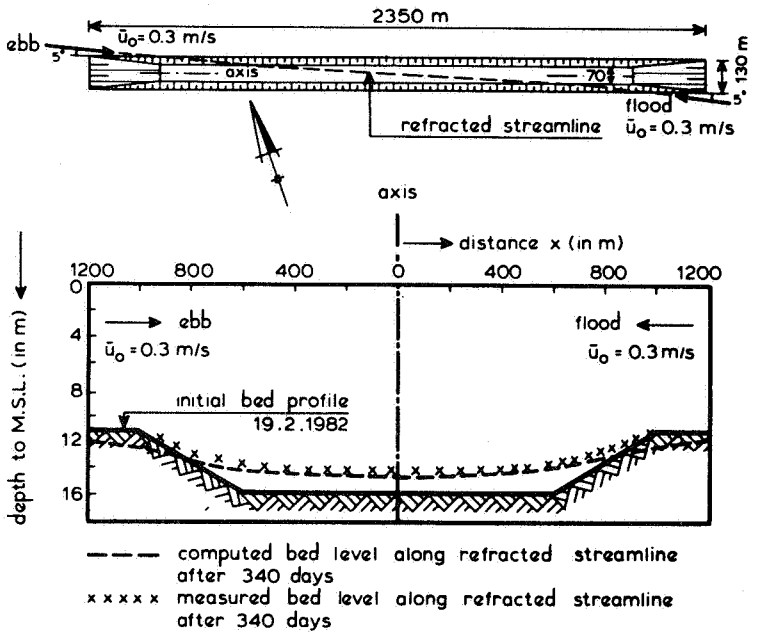

FIG. 10.—Siltation in Trial Dredge Channel near Bahia Blanca, Argentina

of 85 mg/L. Because the bed material consisted (for 80%) of silty materials, the bed-boundary condition cannot be represented by Eq. 14 which is only valid for sandy material. For silty material the following equation is more appropriate:

$$E_a = -\left(\epsilon_s \frac{\partial c}{\partial z}\right)_{z=a} = \alpha_s \left[\frac{\bar{\tau}_b' - \bar{\tau}_{b,cr}}{\bar{\tau}_{b,cr}}\right]^{1.5} \quad \ldots\ldots\ldots\ldots\ldots\ldots\ldots\ldots\ldots\ldots \quad (21)$$

in which α_s = material constant.

The $\bar{\tau}_{b,cr}$ parameter was assumed to be 0.1 N/m^2, which is a typical value for silty material. The α_s parameter was determined by calibration using concentrations measured outside the trial dredge channel. Eq. 21 was applied at a level of a = 0.01 m. The effective bed roughness was assumed to be 0.01 m (almost flat bed). Fig. 10 shows measured and computed bed level profiles after a period of 340 days. The agreement is rather good in the middle section of the channel, where a siltation height of about 1.5 m can be observed. The maximum deviation between measured and computed values in the middle section is about 0.3 m.

The predicted erosion at the side banks was not observed. Probably, the consolidated bed material outside the channel was too stable to be eroded at the governing flow and wave conditions. To model this effect, more information (measurements) of the critical bed-shear stress ($\bar{\tau}_{b,cr}$) must be available.

Practical Graphs for Sedimentation Predictions

Often, it is practical to have a set of simple graphs to get a first estimate of the trapping efficiency of a proposed channel. To obtain such graphs, the SURTRENCH-model was applied to determine the trapping efficiency of dredged channels situated at various angles to the approaching current. A definition sketch is shown in Fig. 11. The channel is assumed to be infinitely long. The current velocities in the channel were computed numerically using Eqs. 18 and 19. The trapping efficiency factor is defined as the relative difference of the incoming suspended load transport and the minimum suspended load transport in the channel, as follows:

$$e = \frac{b_o s_o - b_1 s_{1,\text{minimum}}}{b_o s_o} \quad \ldots\ldots\ldots\ldots\ldots\ldots\ldots\ldots\ldots\ldots\ldots\ldots\ldots\ldots \quad (22)$$

in which b_o = width of approaching streamtube; b_1 = width of streamtube in channel; s_o = incoming suspended load transport per unit width; and s_1 = suspended load transport in channel per unit width.

The basic parameters which determine the trapping efficiency factor, are: the approach angle (α_o), the approach velocity ($\bar{v}_{r,o}$), the approach depth (h_o), the approach bed-shear velocity ($u_{*,o}$), the particle fall velocity (w_s), the wave height (H), the channel depth (d), the channel width (B), the channel side slope (tan γ) and the bed roughness (k_s). The functional relationship can be described as follows:

$$e = F\left(\alpha_o, \bar{v}_{r,o}, \frac{w_s}{u_{*,o}}, \frac{H}{h_o}, \frac{k_s}{h_o}, \frac{d}{h_o}, \frac{B}{h_o}, \tan\gamma\right) \quad \ldots\ldots\ldots\ldots\ldots\ldots\ldots\ldots \quad (23)$$

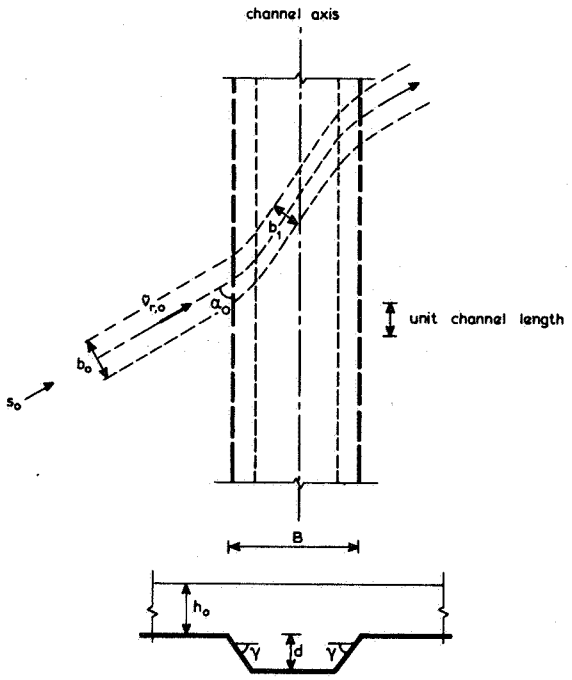

FIG. 11.—Definition Sketch

A sensitivity analysis (18) has shown that the influence of the approach velocity $\bar{v}_{r,o}$, the relative wave height H/h_o and the relative roughness k_s/h_o is relatively small compared with the influence of the other parameters. To reduce the number of computations the former parameters, were therefore not varied. In all, 300 computations were executed, using the following data: approach velocity = $\bar{v}_{r,o}$ = 1 m/s; approach water depth = h_o = 5 m; approach angles = α_o = 15°, 30°, 60°, 90°; channel depth = d = 2, 2.5, 5, 10 m; channel width (normal to axis) = B = 50, 100, 200, 500 m; channel side slope (normal to axis) = tan γ = 0.2, 0.1, 0.05; particle fall velocity = w_s = 0.0021, 0.005, 0.0107, 0.0142, 0.025, 0.036 m/s; and bed roughness = k_s = 0.2 m. The results are presented in Figs. 12 and 13.

As can be observed, the trapping efficiency factor e increases for an increasing approach angle (α_o). The maximum trapping efficiency does occur for α_o = 90°, because there is a maximum reduction of the current velocity in the channel for this situation.

Finally, note that the applicability range of the graphs is limited to the values of the parameters not varied (approach velocity, bed roughness and wave height). Additional computations have been carried out to extend the applicability range of the graphs accepting an error in the trapping efficiency factor of about 25%, which resulted in: $\bar{v}_{r,o}$ = 0.8 to 1.2 m/s, k_s/h = 0.02 to 0.06 and H/h_o = 0 to 0.3. The proposed graphs should be used only when a rough estimate of the sedimentation is considered adequate.

The sedimentation rate (ΔS) per unit channel length (see Fig. 11) immediately after dredging can be computed by:

$$\Delta S = es_o \sin \alpha_o \quad \ldots\ldots (24)$$

As a computation example the following situation is given: α_o = 30°; $\bar{u}_o$ = 1 m/s; h_o = 5 m; $u_{*,o}$ = 0.05 m/s; d = 5 m; tan γ = 0.1; B = 200 m;

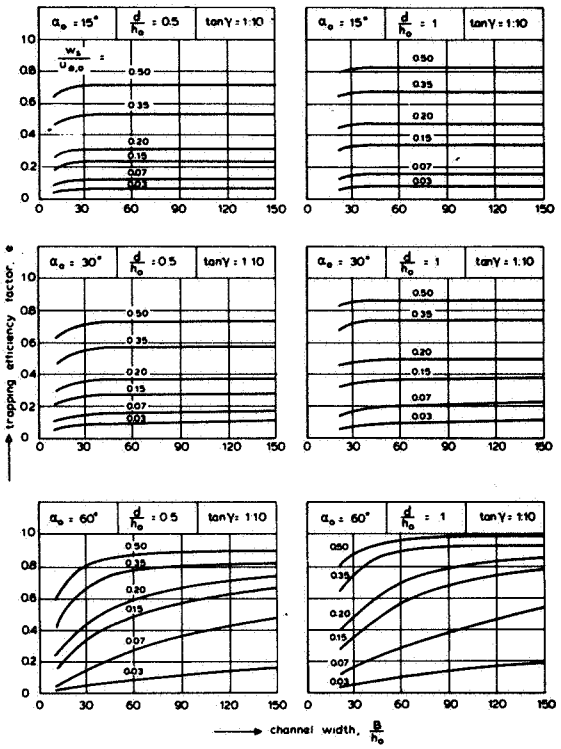

FIG. 12.—Trapping Efficiency Factors for Approach Angle of α_o = 15°, 30°, 60°

and w_s = 0.01 m/s. The dimensionless parameters are: $w_s/u_{*,o}$ = 0.2; d/h_o = 1; B/h_o = 40; yielding trapping efficiency factor $e \simeq 0.5$ (Fig. 12). For an incoming suspended load transport of s_o = 1 kg/sm the sedimentation rate per unit channel length is $\Delta S = 0.5 \times 1 \times \sin(30°) =$

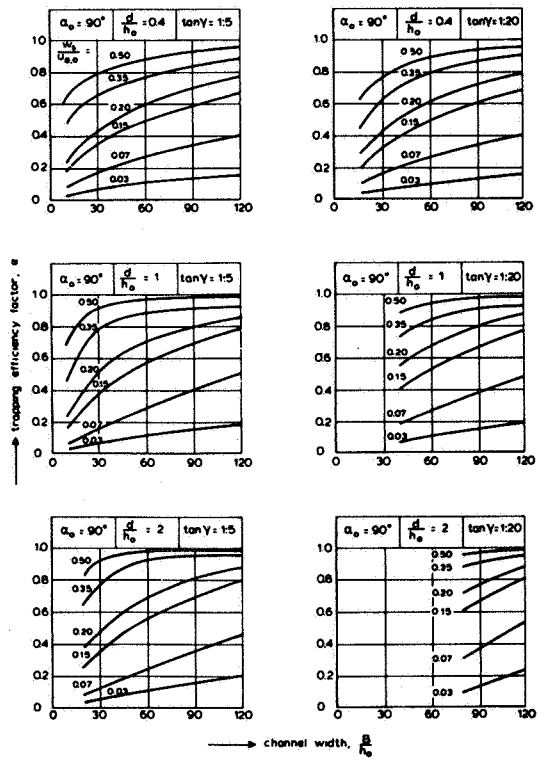

FIG. 13.—Trapping Efficiency Factors for Approach Angle of α_o = 90°

0.25 kg/sm. The total sedimentation (mass) in one month in a channel with a length of 1,000 m is $M_s = (0.25) \times (30 \times 24 \times 3{,}600) \times (1{,}000) = 648\ 10^6$ kg.

Conclusions and Analysis

The study has led to the following conclusions:

1. A mathematical model is presented to compute the suspended sediment transport and sedimentation rates by currents and waves in a dredged channel; comparison of measured and computed sediment concentration profiles and bed level changes shows reasonable agreement.
2. A current approaching an oblique channel is refracted resulting in contraction of the streamlines; the influence of the refraction effect on the sedimentation process is relatively small when the angle between the approaching current and the channel axis is larger than 60°.
3. Waves propagating in a dredged channel are reduced in height due to the increased water depth; the influence of the wave height reduction on the sedimentation process is relatively small; hence, it seems acceptable to apply a constant wave height outside and inside the channel.
4. A set of graphs is presented which can be used to get a rough estimate of the sediment trapping efficiency of dredged channels.

The proposed mathematical model which represents all relevant transport processes such as convection, diffusion, settling and sediment pick-up should be more accurate to predict the sedimentation rate of a dredged channel than previously presented models (3, 4, 11 and 12), which are based on a rather strong schematization of the transport processes. Some of these latter methods are highly empirical. Furthermore, most of these methods have been derived for channels that are situated approximately perpendicular ($\alpha \simeq 90°$) to the current direction and have, therefore, a rather restricted application range.

The advantages of the more sophisticated mathematical approach may disappear, however, when there is no accurate information of the boundary conditions such as the future currents and waves outside the channel. When the dredging volume is critical in the economic feasibility of the entire project, a large effort is usually made to determine the boundary conditions by performing field measurements (automatic current recordings, wave rider buoys) and by applying two-dimensional horizontal flow and wave propagation models. In this latter case the application of the proposed mathematical model to predict the sedimentation rate is fully justified. When detailed information of the boundary conditions is lacking, an accurate estimation of the sedimentation rate cannot be obtained by any model. In that case the simple sedimentation formulas or graphs are adequate.

Appendix.—References

1. Bakker, W. T., and Doorn, T. van, "Near-Bottom Velocities in Waves with a Current," *Proc.*, 16th Conf. on Coastal Eng., Vol. 2, Paper 110, Hamburg, W. Germany, 1978.

2. Boer, S., "The Flow across Trenches at Oblique Angle to the Flow," Report S 490, Delft Hydraulics Laboratory, Delft, The Netherlands, 1985.
3. Bijker, E., "Sedimentation in Channels and Trenches," *Proc.*, 17th Conf. on Coastal Eng., Sydney, Australia, 1980, pp. 299–300.
4. Eysink, W., and Vermaas, H., "Computational Method to Estimate the Sedimentation in Dredged Channels and Harbour Basins in Estuarine Environments," Int. Conf. on Coastal and Ports Eng. in Developing Countries, Colombo, Sri Lanka, 1983.
5. Wallingford, H. R. S., "Laboratory Studies of Flow across Dredged Trenches," *Report EX 618*, Wallingford, England.
6. Jonsson, I. G., "Energy Flux and Wave Action in Gravity Waves Propagating on a Current," *Journal of Hydraulic Research*, Vol. 16, No. 3, 1978, pp. 223–234.
7. Kemp, P. H., and Simons, R. R., "The Interaction of Waves and a Turbulent Current: Waves Propagating with the Current," *Journal of Fluid Mechanics*, Vol. 116, 1982, pp. 227–250.
8. Kemp, P. H., and Simons, R. R., "The Interaction of Waves and a Turbulent Current: Waves Propagating against the Current," *Journal of Fluid Mechanics*, Vol. 130, 1983, pp. 73–89.
9. Kerssens, P. J. M., and Rijn, L. C. van, "Model for Non-Steady Suspended Sediment Transport," *Proc.*, 18th IAHR-Congress, Vol. 1, Baden-Baden, W. Germany, 1977, pp. 113–121.
10. Kerssens, P. J. M., Prins, A., and Rijn, L. C. van, "Model for Suspended Sediment Transport," *Journal of the Hydraulics Division*, ASCE, HY5, 1979, pp. 461–476.
11. Lean, G. H., "Estimation of Maintenance Dredging for Navigation Channels," H. R. S. Wallingford, England, 1980, p. 15.
12. Mayor-Mora, R., Mortensen, P., and Fredsøe, J., "Sedimentation Studies on the Niger River Delta," *Proc.*, 15 Conf. on Coastal Engrg., Honolulu, Hawaii, 1976, pp. 2151–2170.
13. Republic of Argentina, Ministerio de Economica, "Dredging Study of the Access Channel to the Port of Bahia Blanca," Buenos Aires, Argentina, 1984.
14. Rijn, L. C. van, "Model for Sedimentation Predictions," *Proc.*, 19th IAHR-Congress, Vol. 2, New Delhi, India, 1980, pp. 321–329.
15. Rijn, L. C. van, "Sediment Transport, Part I: Bed Load Transport," *Journal of Hydraulic Engineering*, Vol. 110, No. 10, 1984, pp. 1431–1456.
16. Rijn, L. C. van, "Sediment Transport, Part II: Suspended Load Transport," *Journal of Hydraulic Engineering*, Vol. 110, No. 11, 1984, pp. 1613–1641.
17. Rijn, L. C. van, "Sediment Transport, Part III: Bed Forms and Alluvial Roughness," *Journal of Hydraulic Engineering*, Vol. 110, No. 12, 1984, pp. 1733–1754.
18. Rijn, L. C. van, "Two-Dimensional Vertical Mathematical Model for Suspended Sediment Transport by Currents and Waves," *Report S 488-IV*, Delft Hydraulics Laboratory, Delft, The Netherlands, 1985.
19. Rijn, L. C. van, "Initiation of Motion, Bed Forms, Bed Roughness, Sediment Concentrations and Transport by Currents and Waves," *Report S 487-IV*, Delft Hydraulics Laboratory, Delft, The Netherlands, 1985.
20. Rijn, L. C. van, "Flume Experiments of Sedimentation in Channels by Currents and Waves," *Report S 347-II*, Delft Hydraulics Laboratory, Delft, The Netherlands, 1985.
21. Vreugdenhil, C. B., "Numerical Solution of a Convection-Diffusion Equation Using Finite Elements," Note X 59, Delft Hydraulics Laboratory, Delft, The Netherlands, 1982.
22. Weide, J. van der, Overeem, J. van, and Doorn, J. T. M., "Recent Developments in Research on the Design and Operational Use of Navigation Channels," Proc. Seatec-Portec Congress, Djakarta, Indonesia, 1985.